

Published in final edited form as:

Science. 2012 March 9; 335(6073): 1232–1235. doi:10.1126/science.1217869.

## Triggering a Cell Shape Change by Exploiting Pre-Existing Actomyosin Contractions

Minna Roh-Johnson<sup>\*,1</sup>, Gidi Shemer<sup>\*,1</sup>, Christopher D. Higgins<sup>1</sup>, Joseph H. McClellan<sup>1</sup>, Adam D. Werts<sup>1</sup>, U. Serdar Tulu<sup>2</sup>, Liang Gao<sup>3</sup>, Eric Betzig<sup>3</sup>, Daniel P. Kiehart<sup>2</sup>, and Bob Goldstein<sup>1,+</sup>

<sup>1</sup>Biology Department, University of North Carolina at Chapel Hill, Chapel Hill, NC, USA

<sup>2</sup>Department of Biology, Duke University, Durham NC, USA

<sup>3</sup>Janelia Farm Research Campus, Howard Hughes Medical Institute, Ashburn, Virginia, USA

### Abstract

Apical constriction changes cell shapes, driving critical morphogenetic events including gastrulation in diverse organisms and neural tube closure in vertebrates. Apical constriction is thought to be triggered by contraction of apical actomyosin networks. We found that apical actomyosin contractions began before cell shape changes in both *C. elegans* and *Drosophila*. In *C. elegans*, actomyosin networks were initially dynamic, contracting and generating cortical tension without significant shrinking of apical surfaces. Apical cell-cell contact zones and actomyosin only later moved increasingly in concert, with no detectable change in actomyosin dynamics or cortical tension. Thus, apical constriction appears to be triggered not by a change in cortical tension but by dynamic linking of apical cell-cell contact zones to an already contractile apical cortex.

---

During development, dramatic rearrangements of cells and epithelia play key roles in shaping animals [1–4]. Many rearrangements are driven by apical constriction, including neural tube closure [4], failure of which is a common human birth defect [5]. Apical constriction is generally driven by contraction of apical actomyosin networks [4]. However, it is not well understood how the stresses and tensions generated by actomyosin networks produce cell shape changes in developing organisms [6].

To address this issue, we examined cortical actomyosin dynamics during *C. elegans* gastrulation. In *C. elegans*, two endodermal precursor cells (Ea and Ep) internalize by apical constriction [7–9]. Transgenic green fluorescent protein (GFP) myosin II-containing particles formed in each cell's apical cortex, enriched in Ea/p similarly to endogenous myosin [9]. The ability to resolve large numbers of particles made it possible to track the detailed dynamics of actomyosin networks (Fig. 1A; Fig. S1; Movie S1). Neighboring myosin particles moved short distances toward each other into multiple coalescence points, with most particles moving centripetally (toward the center of the apical cell surface), and with new particles forming near apical cell boundaries (Fig. 1B; Fig. S2). These particles appear to be components of contracting actomyosin networks, because F-actin coalesced similarly (Fig. S2), and myosin particles near the center of each coalescence moved at a

---

<sup>\*</sup>to whom correspondence should be addressed. bobg@unc.edu, phone 919 843-8575.

<sup>+</sup>These authors contributed equally to this work

Data reported in this paper are presented in the main paper and in the supporting online material.

The authors declare no conflicts of interest.

slower speed than those further away (Fig. S3) as seen in other contracting actomyosin networks [10]. Particle tracking and fluorescence recovery after photobleaching (FRAP) experiments suggested that the networks were continuously remodeled by exchange of myosin molecules on and off particles as expected (Fig. S3).

To investigate how apical actomyosin networks shrink apical cell surfaces, we tracked the outlines of these surfaces, the apical cell-cell contact zones, quantitatively (Fig. 1C–D). Apical areas shrunk gradually or not at all at first (Fig. 1D–F) [11] and then accelerated. We predicted that actomyosin contraction would also begin gradually and accelerate in concert with the contact zones (Fig. 1E). Instead, myosin particles moved centripetally quite rapidly throughout this period (Fig. 1F;  $3.19 \pm 0.14 \mu\text{m}/\text{min}$ , mean  $\pm$  95% CI), at first with little or no accompanying contact zone movement. Myosin particles near contact zones at first streamed away from the contact zones, which were in many cases almost stationary, suggesting that the actomyosin network and contact zones were only weakly mechanically connected at this stage (Fig. 1G; Movies S2, S3; we refer to actomyosin contractions without contact zone movement as uncoupled movements). Later, contact zones appeared to move almost in unison with many of the myosin particles (Fig. 1G; Movie S4; referred to as coupled movements), suggesting that the myosin and contact zones may have become mechanically connected. Contact zones were never seen to overtake myosin particles in the Ea/p cortex (Movies S2–5), suggesting that neighboring cells were not simply migrating over Ea/p cells.

Our observations were not entirely consistent with a simple pattern of uncoupled movements early and coupled movements later (Fig. S4); instead, some variation existed at each stage. Tracking movements by particle image velocimetry (PIV) demonstrated that in general, the myosin particles and contact zones moved increasingly in unison as time progressed (Fig. 1H). We confirmed this result by measuring the rates of individually tracked myosin particles and nearby contact zones, defining the difference between these two rates as a slipping rate (Fig. 1I). Actomyosin contractions appeared to drive contact zone movements with ~25% efficiency in early stages, increasing to ~81% efficiency near the end of Ea/p internalization, based on comparing measurements from cells with a computer simulation (Fig. S5; Movie S6). Labeling cell surfaces with Quantum Dots or a plasma membrane marker demonstrated that cell surfaces moved in concert with underlying actomyosin network contractions; i.e. there may be strong frictional force or drag force between the actomyosin network and the overlying plasma membrane (Fig. S6). Thus, slipping between actomyosin and membrane occurred specifically at apical cell contact zones, and the relationship between cytoskeletal dynamics and cell shape change during apical constriction is more dynamic than existing models [3, 4] predict.

To determine if the phenomenon we found is conserved in other systems, we examined *Drosophila* ventral furrow cells [11], in which periodic actomyosin contractions cause apical cross-sectional profiles to shrink in pulses [12]. We noticed myosin accumulations in some cells even before shrinking of apical profiles began (Fig. 2A). Myosin coalesced and moved either toward or away from stationary membranes, and thus was not well connected to contact zone movements at first (Fig. 2B; Movie S7). One or more rounds of myosin enrichment and dissipation occurred in most cells (89%; n=55) before apical profiles began to shrink (Fig. 2C–E). These early actomyosin contractions occurred periodically, with a time interval of  $75 \pm 24\text{s}$ , similar to that previously measured just after this stage, during apical constriction [12]. Some of the early contractions might contribute to cell surface flattening in *Drosophila*, because apical surfaces are not yet completely flattened at this stage [13], although many early contractions were not centripetally directed (Fig. 2B). Myosin moved at a faster rate than did nearby contact zones at first, and this difference was significantly reduced later, as also observed in *C. elegans* (Fig. 2F). Thus, the early

activation of actomyosin contraction, before apical cell profiles begin to shrink, might be a conserved feature of apical constriction.

We hypothesized that a change in the apparent efficiency of actomyosin-contact zone connections suggested by our *C. elegans* results might be a secondary effect of changes in viscoelastic properties, for example stiffening or softening of actomyosin networks in contracting cells or their neighbors. We tested this in two ways. First, we analyzed a naturally occurring phenomenon. The apical networks in Ea/p cells occasionally failed spontaneously, with centripetally moving myosin particles suddenly springing away from one another (Fig. 3A). During recoil, myosin particle movements slowed exponentially, suggesting that the apical cortex behaves as a viscoelastic network [14–16], and initial recoil speeds and their exponential decays were similar between early and late stages, suggesting little change in cortical tension or stiffness of the network over time [15, 17] (Fig. 3B). Second, we cut the cortical actomyosin network using a focused UV laser beam and measured initial recoil speed as a quantitative estimate of tension in the network [18–23]. The cortical network recoiled rapidly from cuts in Ea/p (Fig. 3B,C), again with little change in initial recoil speed between early and late stages (Fig. 3B). Cutting a neighboring cell's cortex produced a recoil that also did not change significantly over time, and that was slower than in Ea/p (Fig. 3B), suggesting that network tension is lower in this cell. Thus, the large difference in the degree of coupled movement between early and late stages is accompanied by little measurable difference in the viscoelastic properties of cortical networks. These results reveal that the cortical tension associated with apical constriction (Fig. 3D) is established well before apical constriction begins, and suggest that the differences between early and late stages might be explained by a change in efficiency of actomyosin-contact zone connections alone.

These results support a picture in which a continuously coalescing apical actomyosin network adds little cortical tension as it begins to move apical cell contact zones, i.e. the tension involved in coalescing the apical actomyosin network is great compared to the small additional tension required to pull contact zones. Although this model may appear counterintuitive, it is in fact consistent with estimates of forces in other biological systems on this size scale [19, 24].

Our results build a model of apical constriction in which the relevant cytoskeletal dynamics can run constitutively, transitioning to driving rapid cell shape change at a later time. We speculate that there may exist in this system a molecular clutch – a regulatable, molecular connection between actomyosin networks and contact zones, transmitting the forces generated by actomyosin contraction to the contact zones. Molecular clutches coordinate actin dynamics and adhesion formation in migrating growth cones and cultured cells [25]. Our results raise the possibility that there might be developmentally regulated clutches functioning in epithelial morphogenesis. Indeed, targeting a cadherin-catenin complex and a Rac pathway prevented the transition to coupled movements, genetically separating coupled movements from contractions in this system (Fig. 4, Figs. S7–9). Thus, cadherin-catenin complex members, Rac pathway targets, or proteins that function alongside either might contribute to a clutch. Temporal regulation of actin nucleators at contact zones could also function as a clutch, if actin polymerized in a centripetal direction from contact zones primarily at early stages. In either model, gradual engagement of a clutch would stabilize connections between a contracting actomyosin network and cell-cell boundaries. Alternatively, resistance to a slipping clutch could change over time, for example because neighboring cells lose tension. This alternative appears unlikely because we detected no change in neighboring cell tension over time. Instead, we speculate that the degree of engagement of a molecular clutch might determine the rate of apical shrinking. As apical

shrinking proceeds, this rate might be limited additionally by the rate at which apical membrane can be removed [26].

Recent work has highlighted a number of actomyosin-based mechanisms that drive cell shape changes in morphogenesis [21, 27, 28]. Periodic contractions of actomyosin networks, flows of actomyosin, and an actomyosin-based ratchet make contributions to changing cell shapes [12, 23, 29, 30]. Here we found that the actomyosin contractions and cortical tension associated with a cell shape change are established even before the cell shape change begins. Thus, the immediate trigger for apical constriction is not the activation of actomyosin contractions or a change in cortical tension, which highlights the dynamic nature of the connections between the actomyosin cytoskeleton and the sites of cell-cell adhesion as a key area of interest for understanding morphogenesis mechanisms.

## Supplementary Material

Refer to Web version on PubMed Central for supplementary material.

## Acknowledgments

We thank K. Bloom, G. Edwards, J. Iwasa, J. Johnson, E. Munro, M. Peifer, D. Reiner, S. Rogers and members of the Goldstein lab for comments on the manuscript, B. Eastwood and R. Taylor for help with particle image velocimetry, J. Fricks for help with statistical analysis, and A. Martin and E. Wieschaus for providing fly strains and sharing movies. This work was supported by NIH R01 GM083071 to BG, NIH R01 GM33830 to DPK, and an HFSP postdoctoral fellowship to GS.

## References and Notes

1. Friedl P, Gilmour D. Collective cell migration in morphogenesis, regeneration and cancer. *Nat Rev Mol Cell Biol.* 2009; 10(7):445–457. [PubMed: 19546857]
2. Weijer CJ. Collective cell migration in development. *J Cell Sci.* 2009; 122(Pt 18):3215–3223. [PubMed: 19726631]
3. Odell GM, et al. The mechanical basis of morphogenesis. I. Epithelial folding and invagination. *Dev Biol.* 1981; 85(2):446–462. [PubMed: 7196351]
4. Sawyer JM, et al. Apical constriction: a cell shape change that can drive morphogenesis. *Dev Biol.* 2010; 341(1):5–19. [PubMed: 19751720]
5. Copp AJ, Greene ND. Genetics and development of neural tube defects. *J Pathol.* 2010; 220(2):217–230. [PubMed: 19918803]
6. Grill SW. Growing up is stressful: biophysical laws of morphogenesis. *Curr Opin Genet Dev.* 2011; 21(5):647–652. [PubMed: 21982413]
7. Lee JY, Goldstein B. Mechanisms of cell positioning during *C. elegans* gastrulation. *Development.* 2003; 130(2):307–320. [PubMed: 12466198]
8. Lee JY, et al. Wnt/Frizzled signaling controls *C. elegans* gastrulation by activating actomyosin contractility. *Curr Biol.* 2006; 16(20):1986–1997. [PubMed: 17055977]
9. Nance J, Priess JR. Cell polarity and gastrulation in *C. elegans*. *Development.* 2002; 129(2):387–397. [PubMed: 11807031]
10. Munro E, Nance J, Priess JR. Cortical flows powered by asymmetrical contraction transport PAR proteins to establish and maintain anterior-posterior polarity in the early *C. elegans* embryo. *Dev Cell.* 2004; 7(3):413–424. [PubMed: 15363415]
11. Materials and methods are available as supporting material on *Science* Online 1
12. Martin AC, Kaschube M, Wieschaus EF. Pulsed contractions of an actin-myosin network drive apical constriction. *Nature.* 2009; 457(7228):495–499. [PubMed: 19029882]
13. Dawes-Hoang RE, et al. folded gastrulation, cell shape change and the control of myosin localization. *Development.* 2005; 132(18):4165–4178. [PubMed: 16123312]

14. Fabry B, et al. Scaling the microrheology of living cells. *Phys Rev Lett*. 2001; 87(14):148102. [PubMed: 11580676]
15. Mayer M, et al. Anisotropies in cortical tension reveal the physical basis of polarizing cortical flows. *Nature*. 2010; 467(7315):617–621. [PubMed: 20852613]
16. Wottawah F, et al. Optical rheology of biological cells. *Phys Rev Lett*. 2005; 94(9):098103. [PubMed: 15784006]
17. Toyama Y, et al. Apoptotic force and tissue dynamics during *Drosophila* embryogenesis. *Science*. 2008; 321(5896):1683–1686. [PubMed: 18802000]
18. Fernandez-Gonzalez R, et al. Myosin II dynamics are regulated by tension in intercalating cells. *Dev Cell*. 2009; 17(5):736–743. [PubMed: 19879198]
19. Hutson MS, et al. Forces for morphogenesis investigated with laser microsurgery and quantitative modeling. *Science*. 2003; 300(5616):145–149. [PubMed: 12574496]
20. Kiehart DP, et al. Multiple forces contribute to cell sheet morphogenesis for dorsal closure in *Drosophila*. *J Cell Biol*. 2000; 149(2):471–490. [PubMed: 10769037]
21. Martin AC, et al. Integration of contractile forces during tissue invagination. *J Cell Biol*. 2010; 188(5):735–749. [PubMed: 20194639]
22. Rauzi M, et al. Nature and anisotropy of cortical forces orienting *Drosophila* tissue morphogenesis. *Nat Cell Biol*. 2008; 10(12):1401–1410. [PubMed: 18978783]
23. Solon J, et al. Pulsed forces timed by a ratchet-like mechanism drive directed tissue movement during dorsal closure. *Cell*. 2009; 137(7):1331–1342. [PubMed: 19563762]
24. Grill SW, et al. Polarity controls forces governing asymmetric spindle positioning in the *Caenorhabditis elegans* embryo. *Nature*. 2001; 409(6820):630–633. [PubMed: 11214323]
25. Mitchison T, Kirschner M. Cytoskeletal dynamics and nerve growth. *Neuron*. 1988; 1(9):761–772. [PubMed: 3078414]
26. Lee JY, Harland RM. Endocytosis is required for efficient apical constriction during *Xenopus* gastrulation. *Curr Biol*. 2010; 20(3):253–258. [PubMed: 20096583]
27. Kasza KE, Zallen JA. Dynamics and regulation of contractile actin-myosin networks in morphogenesis. *Curr Opin Cell Biol*. 2011; 23(1):30–38. [PubMed: 21130639]
28. Lecuit T, Lenne PF, Munro E. Force generation, transmission, and integration during cell and tissue morphogenesis. *Annu Rev Cell Dev Biol*. 2011; 27:157–184. [PubMed: 21740231]
29. He L, et al. Tissue elongation requires oscillating contractions of a basal actomyosin network. *Nat Cell Biol*. 2010; 12(12):1133–1142. [PubMed: 21102441]
30. Rauzi M, Lenne PF, Lecuit T. Planar polarized actomyosin contractile flows control epithelial junction remodelling. *Nature*. 2010; 468(7327):1110–1114. [PubMed: 21068726]

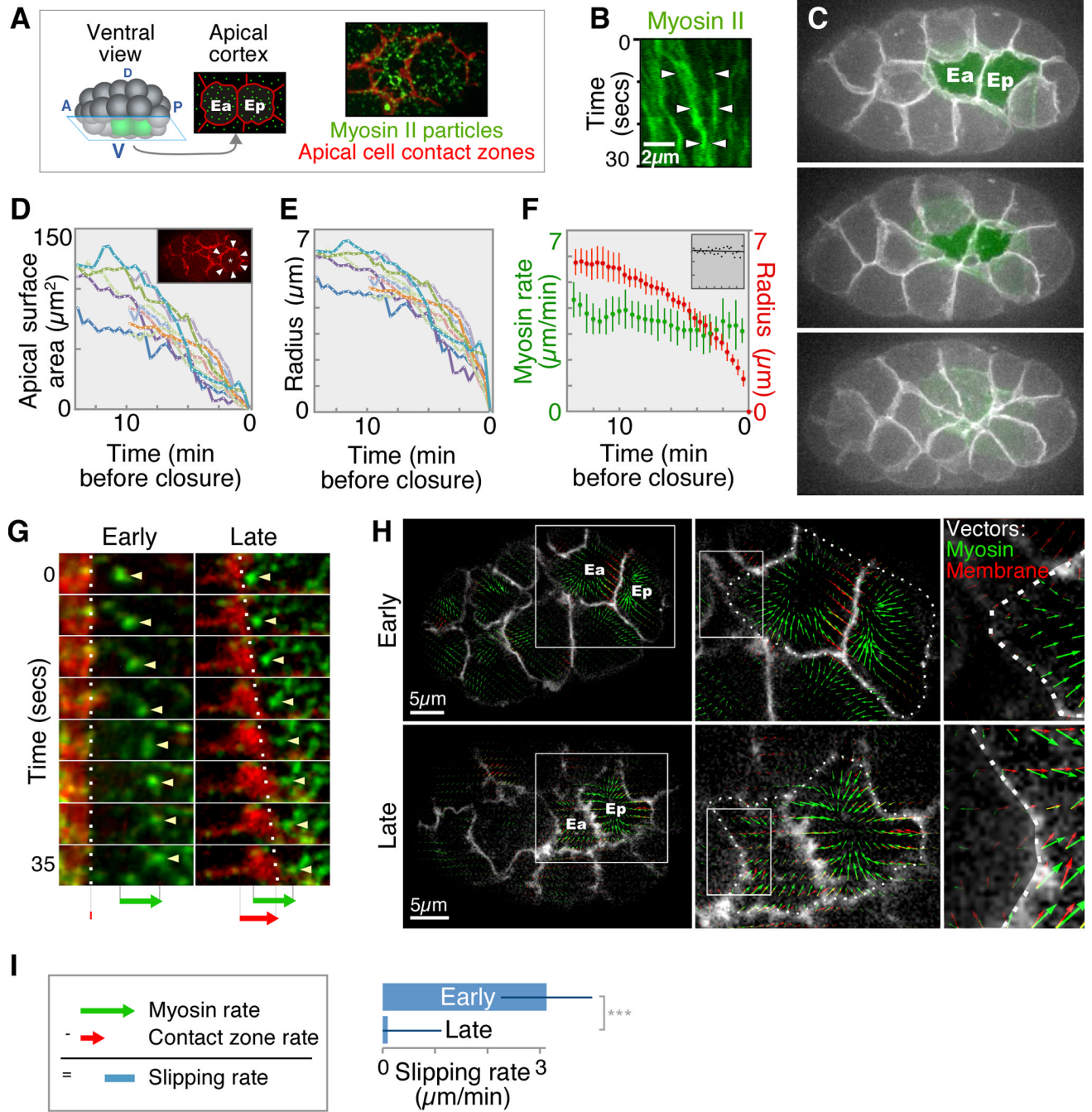


**Figure 1. Actomyosin contraction precedes the rapid shrinking of the apical surface**  
 (A) Diagram of imaging method. (B) NMY-2::GFP coalescence (white arrowheads) in apical cortex of Ea/p cell. (C) Shrinking of apical surfaces during gastrulation (projections of ten 1 $\mu$ m z-planes, with Ea/p false-colored). (D) Ea/p cell apical surface areas over 575 or 825 secs (5 embryos each) before closure of the apical surface. Inset: apical cell-cell contact zones (arrowheads) on Ep (asterisk). (E) Average radius of apical surfaces derived from area measurements. (F) Mean and 95%CI of radius and myosin particle rate over time. Inset: myosin directionality (net distance over total distance, vertical scale 0 to 1) over time (time scale: same as larger graph). (G) Movements of individual myosin particles (arrowheads) near contact zones (white dotted lines) in early or late stages of closure. Arrows at bottom:

relative distances traveled by each. (H) PIV, three magnifications. Boxes indicate enlarged areas. Left to right: whole embryo at plane of Ea/p apical cortex, Ea/p cells (outlined by dotted line), part of Ea at border with another cell. (I) Slipping rate calculated from individual particles and contact zones ( $p < 0.001$ , Student's t-test).

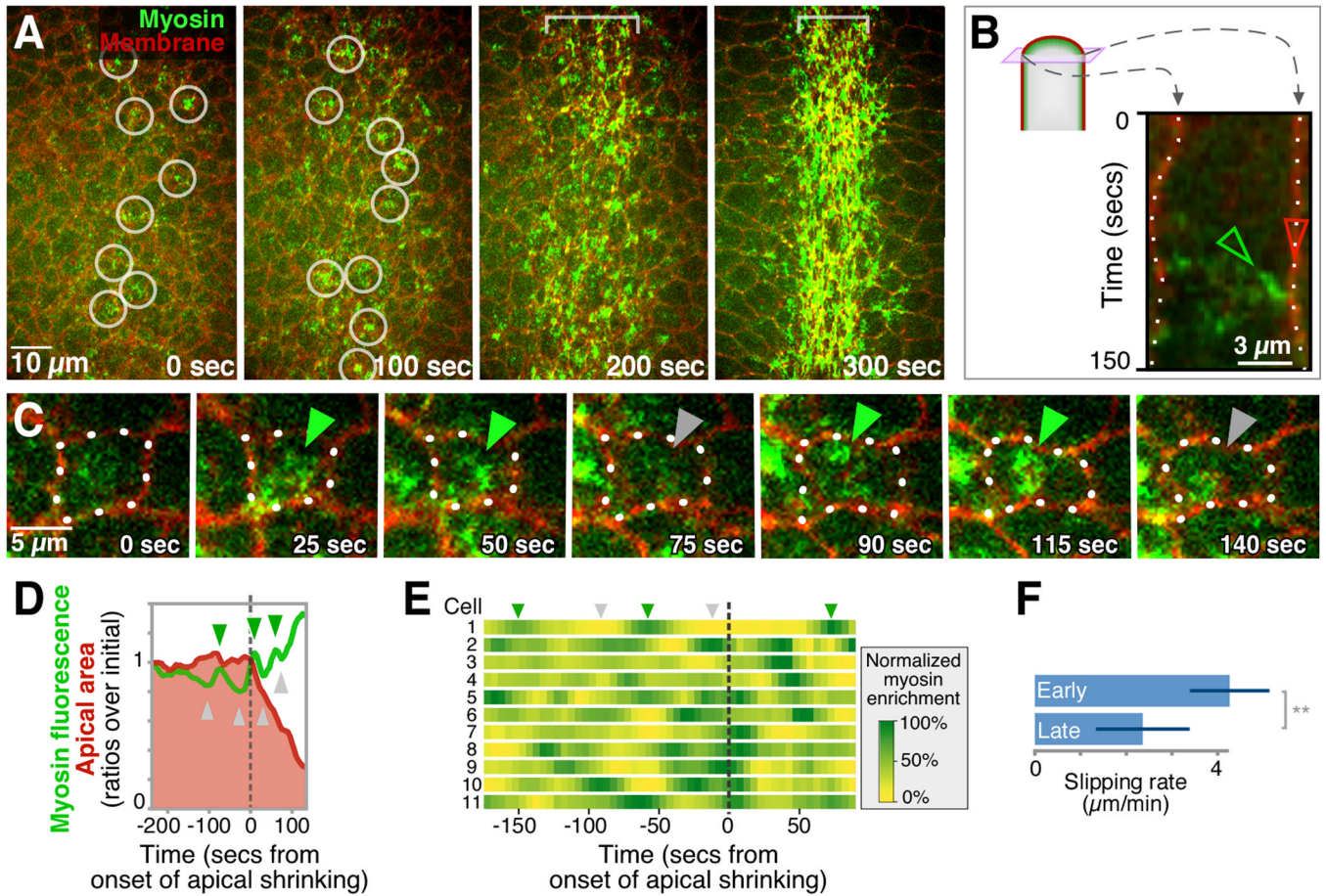


**Figure 2. Periodic actomyosin coalescence occurs before apical cell profiles shrink in *Drosophila* gastrulation**

(A) *Drosophila* ventral furrow formation. Circles mark apical myosin enrichment seen before apical cell profiles began to shrink. (B) Kymograph of a cell (diagrammed) showing myosin (green) movement toward a stationary cell-cell boundary (red) before apical shrinking began. (C) Myosin coalesced (green arrowheads) and dissipated (gray arrowheads) before apical cell profiles began to shrink. This is shown quantitatively from one cell in (D), and from 11 cells chosen at random in (E). Heatmaps in (E) show local maxima of apical myosin levels (3-timepoint running averages of myosin level at each timepoint minus the average of 10 timepoints before and after, normalized to maximum and minimum). Green and gray arrowheads mark one case as in (C). Cell 3 is a rare example where peaks were not seen before apical shrinking began. (F) Slipping rate, defined as in Fig. 1I, early (before apical shrinking,  $n=33$  cells, 3 embryos) and late (during apical shrinking,  $n=27$  cells, 3 embryos),  $p<0.01$  (Student's t-test).



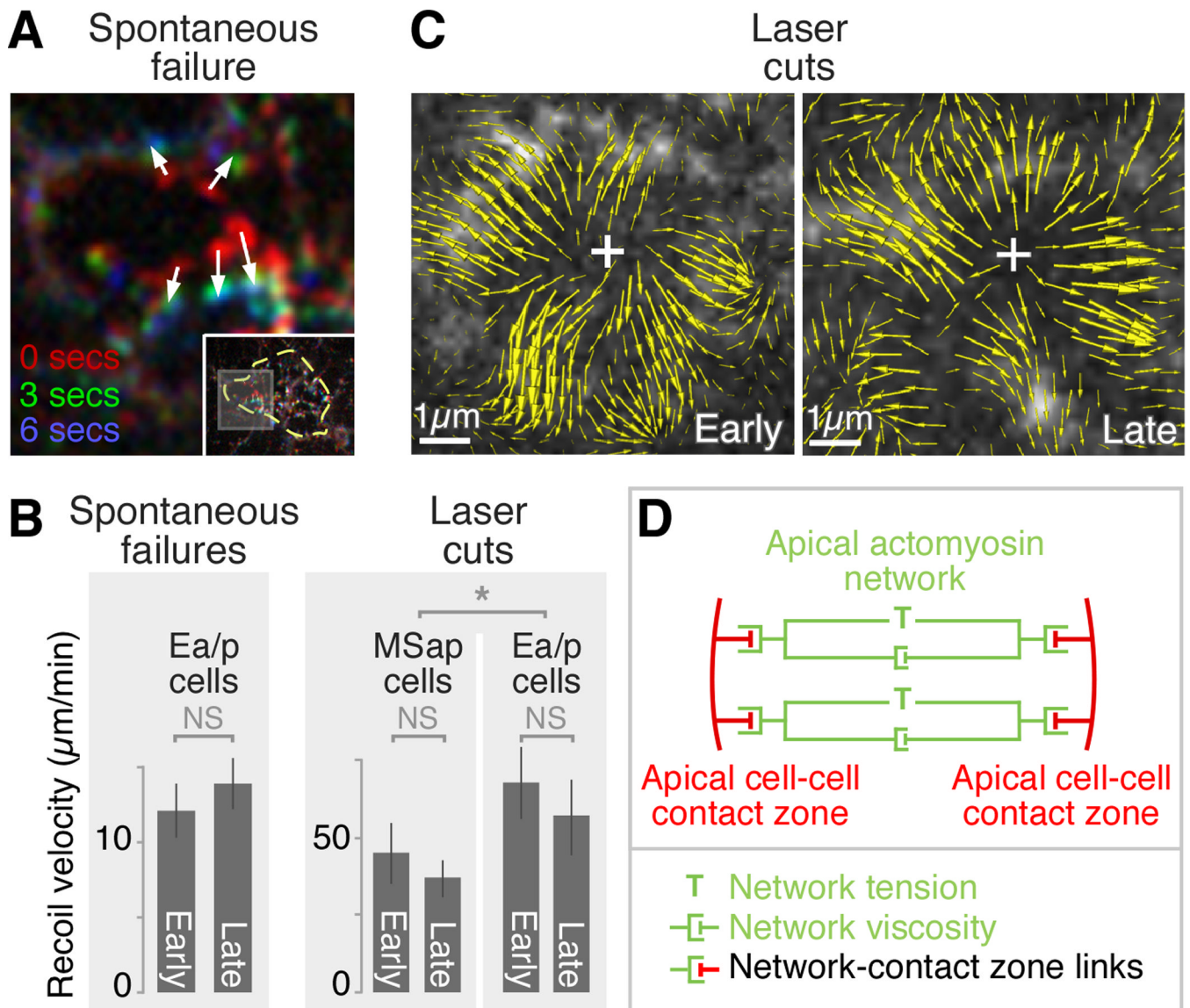


**Figure 3. Cortical tension associated with apical constriction is established early and changes little as apical shrinking accelerates in *C. elegans***

(A) A spontaneous failure, with three timepoints overlain in three colors. Inset shows entire Ea/p cell apical cortex outlined with enlarged region indicated. Arrows mark individual myosin particles springing apart. (B) Similar data from Ea/p cortical laser cuts done in early or late stages by PIV as in Fig 1H. (C) Initial recoil speeds of myosin particles after spontaneous failures at early ( $n=13$  myosin particles within  $1\mu\text{m}$  of center of recoil, 6 embryos) and late (20 particles, 7 embryos) stages, or after laser cuts (48 particles within  $4\mu\text{m}$  of cut site, 7 embryos/stage). Exponential decay  $T_{1/2}$  was 2.20 secs in early stages,  $n=12$ ; 2.38 secs in late stages,  $n=20$ . (D) Working model of forces acting on contact zones (red) and within Ea/p apical actomyosin networks (green, with multiple, interconnected network elements represented as two elements here for simplicity). Results suggest that cortical tension (T) and network stiffness or viscous drag (green dashpots) within Ea/p change little from early to late stages.

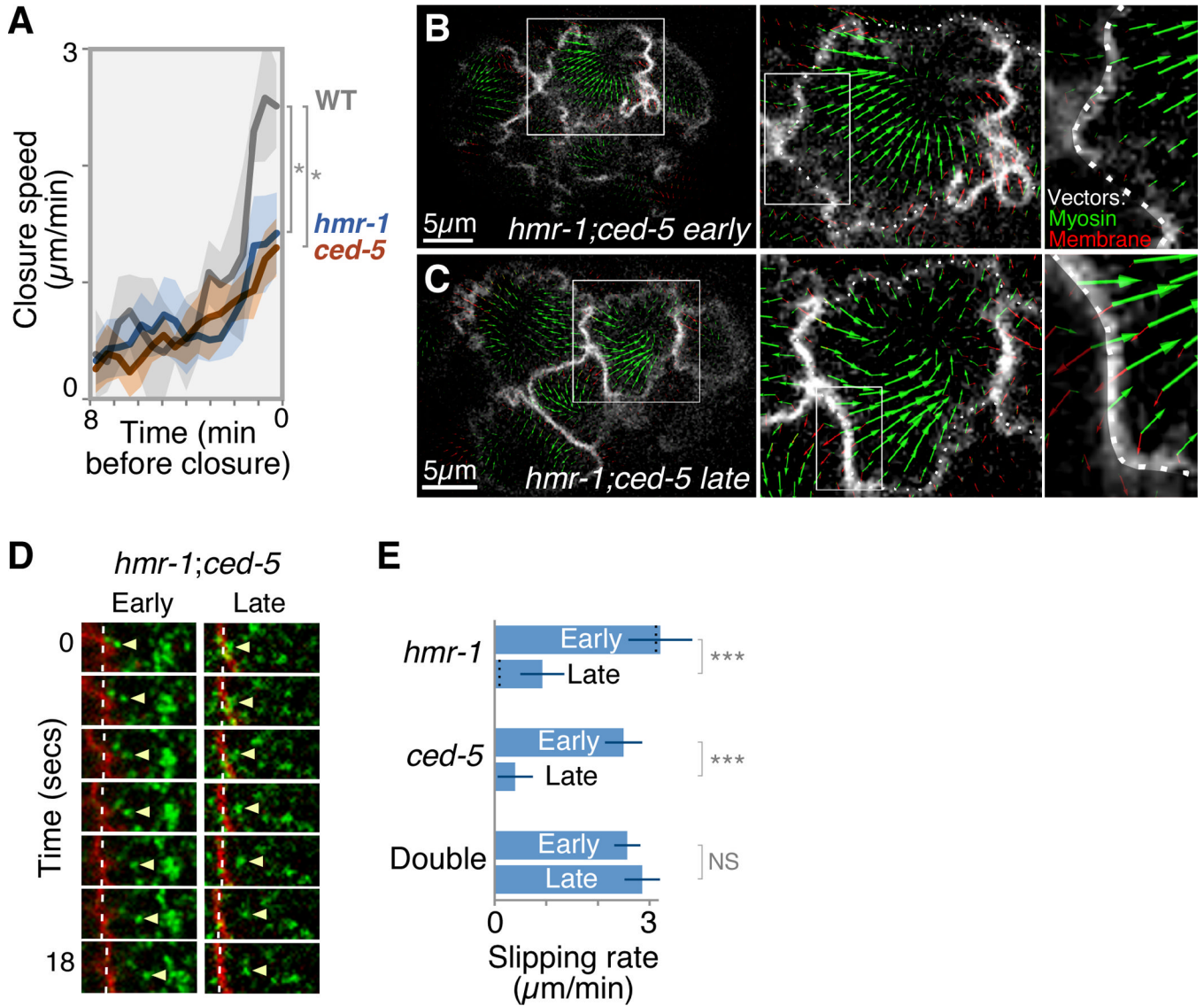


**Figure 4. Targeting classical cadherin and Rac signaling prevents coupled movements but not actomyosin contraction**

(A) Closure speed ( $\mu\text{m}/\text{min}$  decrease in average diameter) of apical cell areas in *hmr-1(RNAi)* or *ced-5(n1812)* does not reach the speed found in wild-type embryos (asterisks:  $p < 0.05$ ). (B) PIV in *hmr-1(RNAi);ced-5(n1812)* doubles. Myosin moves centripetally with little membrane movement in the same direction at either stage. This is shown for individual particles in (D), with quantification as in Fig. 11 in (E). Black dotted lines on *hmr-1* bars in (E) mark wild type for comparison. Asterisks:  $p < 0.001$  (Student's t-test).